



Reduced effective sensitivity of Acoustoelectric Tomography

Ben Keeshan¹, Andy Adler¹, Carlos Rossa¹

¹Systems and Computer Engineering, Carleton University, Ottawa, Canada

Correspondence : Ben Keeshan, e-mail : benkeeshan@cmail.carleton.ca

Abstract- Acoustoelectric tomography is a promising hybrid imaging technique that exploits the coupled physical effect of electrical impedance tomography and ultrasound excitation. It reconstructs the interior conductivity distribution of the tissue using measurements of the voltage resulting from perturbations in the conductivity induced by the US wave. The acoustoelectric effect has been modelled as a linear coupling between the ultrasound coupling field and the conductivity distribution. The linear conductivity dependence of the acoustoelectric effect competes with the inverse dependence of the electrical impedance tomography sensitivity resulting in a suppression of the expected signal. This paper quantifies this effect using numerical simulations and shows that the conductivity contribution to the forward problem is dominated by the physics of electrical impedance tomography, resulting in a non-linear relationship between the signal and changes to the conductivity.

Keywords: Electrical Impedance tomography; Acoustoelectric tomography; Acoustoelectric Effect

1. Introduction

Electrical impedance tomography (EIT) is an inexpensive, portable, and non-invasive imaging technique with many interesting applications in medical imaging which involves an inherently inverse problem. A hybrid imaging technique which combines ultrasound (US) and EIT is Acoustoelectric Tomography (AET). AET relies on the acoustic electric effect (AEE), which provides additional information about the interior regions of the body and can thus help stabilize the EIT inverse problem. AET pulsates an US wave through the body to perturb a classic EIT measurement, where there are some number of surface electrodes injecting a current and measuring the resultant surface voltages with no interior current sources. The time dependent AEE perturbations in the potential is measured by surface electrodes and can be used to calculate the interior power density, a non-linear function of σ , which is sensitive to the entire interior region. The conductivity can then be reconstructed with higher resolution from the measurements of the power density.

The EIT problem is to use some number of boundary voltage and current measurements and the generalized Laplace equation (which determines the potential, u , given no internal sources of current, if either Dirichlet i.e. specify the potential; or Neumann, i.e. specify the current, boundary conditions are specified) to reconstruct the conductivity $\sigma(x)$.

When the medium is perturbed with a ultrasound pulse, the change to the local conductivity is typically modelled by a linear relation:

$$\sigma_p(\mathbf{x}) = \sigma(\mathbf{x}) + \delta\sigma(\mathbf{x}, t) = (1 + kp(\mathbf{x}, t)) \sigma(\mathbf{x}). \quad (1)$$

Here k is a coupling constant $k = \mathcal{O}(10^{-8}, 10^{-9})\text{Pa}^{-1}$ while $p(\mathbf{x}, t)$ is the pressure at position \mathbf{x} and time t . The perturbed potential, u_p , obeys its own generalized Laplace equation. Maintaining the non-perturbed boundary conditions results in a perturbation in the dissipated power given by:

$$P_d(t) = - \int_{\Omega} \delta\sigma \nabla u(\sigma) \nabla u_p(\sigma_p) dV = k \int_{\Omega} p(\mathbf{x}, t) \sigma \nabla u \nabla u_p dV. \quad (2)$$

Neglecting higher order contributions gives:

$$P_d(t) = -k \int_{\Omega} p(\mathbf{x}, t) \sigma |\nabla u|^2 dV = k \int_{\Omega} p(\mathbf{x}, t) M(\sigma) dV, \quad (3)$$

where $M(\sigma)$ is the power density. Equation 3 is a Fredholm equation of the first kind. The vast majority of the AET literature focuses on the last step of the AET process, reconstructing the conductivity from an assumed known power density (Ammari *et al* 2008; Kuchment P and Kunyansky 2010; Adesokan *et al* 2019). Recently, a more comprehensive method to solve the AET problem has tackled the initial step of solving for the power density (Li *et al* 2020). These methods rely on reconstructing the surface potential, which requires many surface electrodes. Thus, the possibility of a system involving very few electrodes makes an accurate estimation of the boundary surface very difficult. In this case, feasibility of an AET reconstruction depends on the strength of the AEE signal. With this in mind, this paper explores the competition between EIT and AEE effects in a single AET measurement.

2. Methods

Consider a quasi-minimal EIT setup with a single EIT measurement made with two drive electrodes and two measurement electrodes. After discretizing space, the measured voltage of a given electrode of the AEE is given by the matrix equation:

$$\delta V_i^{AEE}(t) = J^{EIT} \delta \sigma = k J_{ij}^{EIT} p(t)_j \sigma_j, \quad (4)$$

where δV_{AEE} is the i^{th} voltage measurement, σ and $p(t)$ are a N dimensional vectors containing the conductivity and pressure for each element in the mesh as a function of time, and $j = 1, 2, \dots, N$.

The time dependence of 4 is discretizing into T time points which yields for a single measurement i :

$$\delta V = k J_{i,j}^{EIT} \sigma_j P_{j,t} = k P \hat{M}, \quad (5)$$

where $\delta V \in \mathcal{R}^{1 \times T}$, $\delta \sigma \in \mathcal{R}^{N \times T}$, and $P_{j,t} = p_j(t)$, $t = 1, 2, \dots, T$ and \hat{M} is a N dimensional vector with j^{th} elements $J_{i,j}^{EIT} \sigma_j$.

A measurement's linear dependence on σ in 5 would naively and mistakenly suggest that the measurement should have a linear dependence on changes to σ . But this linear dependence on σ will compete with the implicit σ dependence of the Jacobian. For a given voxel, the current density is $j = \sigma E$, where E is the electric field. Assuming the current density is locally constant, $E \approx \frac{j}{\sigma}$, this gives:

$$J^{EIT} = \sigma |E|^2 \approx \frac{|j|^2}{\sigma}. \quad (6)$$

Plugging this in turn into Equation (4) with the (unrealistic) assumption of constant current flow gives:

$$\delta V_i \approx k p(t)_j \frac{1}{\sigma_j} \sigma_j. \quad (7)$$

This suggests that while the form of 4 seems to imply a strong proportionality between the local conductivity perturbed by the US and the AEE signal, the dependence of σ on the AEE signal competes with its dependence on EIT. In fact the naive expectation is the exact cancellation of the AEE dependence on the local conductivity. This exact cancellation will not occur as 6 is only a rough approximation resulting in a non-trivial σ dependence.

2.1. Simulation

The simulated phantom is a cylindrical with a height and radius of 1 cm with 4 electrodes attached. The simulated experimental setup is shown in Figure 1. Three different configurations are used to highlight the signal's dependence on the EIT sensitivity, where the electrodes are placed at a height of 2 mm, 5 mm, and 8 mm respectively. The AET forward problem is solved using the finite element method, employing a mesh of 310413 tetrahedral elements. The conductivity is discretized with a less fine mesh of 53398 tetrahedral elements using the Matlab software package EIDORS. We consider 4 different conductivity cases. A homogeneous case, and 3 heterogeneous cases with a background conductivity of 1 and a central cylinder (with a radius of 3 mm and height of 10 mm), central sphere (with a radius of 3mm), and a slightly off-center (centered at (0,0,4) mm) cube (with side length of 6 mm) inclusion respectively. Using 4 attached electrodes, electrodes 1 and 3 are driven with a 1 Amp current while the resultant voltage is measured between 2 and 4. The US wave is simulated using Field-ii (Jensen and Svendsen 1992; Jensen 1996). Field ii is a C-program with a Matlab interface

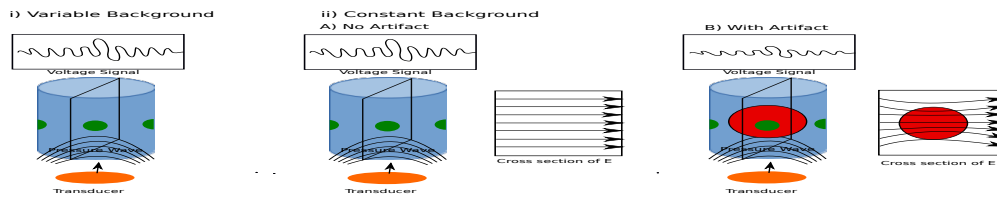


Figure 1: Pictorial representation of the numerical experiments. Two setups are considered: a phantom with an uniform background conductivity simulated with variable conductivity, and a phantom with a constant background conductivity of 1 S/m and a variable inclusion of various shapes which alters the electric field and the internal current flow as illustrated. In each setup an US pressure wave travels through the phantom, generating the AEE signal.

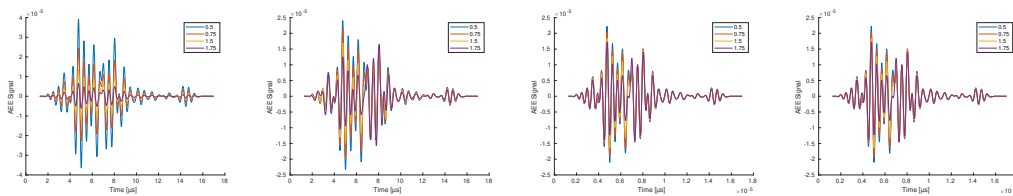


Figure 2: Simulated AEE signal for various conductivity distributions. Left: AEE signal for homogeneous conductivity. Middle left: AEE signal for conductivity with constant background of 1 and a cylindrical inclusion with a variable conductivity. Middle right: AEE signal for conductivity with constant background of 1 and a spherical inclusion with a variable conductivity. Right: AEE signal for conductivity with constant background of 1 and a cubic inclusion with a variable conductivity.

which can easily be interfaced with EIDORS. It does not require an internal spatial mesh in its simulation (instead relying on linear spatial impulse responses). For simplicity the same mesh for the pressure wave and the conductivity are used. It is assumed that the conductivity and the pressure are both constants on each mesh element. A single element concave transducer is simulated with a diameter of 19 mm, a focal length of 300 m with an element size of 1 mm. The excitation consisted of a single period of a 1.6 MHz sinusoid with a Hanning weighting. The excitation was scaled to produce a peak pressure of 2.6 MHz. Our simulated setup is shown in Figure 1. The acoustoelectric coupling constant is set to $k = 10^{-9}$. As EIDORS calculates the EIT Jacobian for a given conductivity mesh, the simulated measured signal can be calculated directly from Equation (5).

3. Results

To investigate the interplay between the EIT sensitivity, the local conductivity, and the AEE signal, the AEE signals are simulated for a variety of different conductivity distributions. Figure 2 shows the effect on the AEE signal from varying the background conductivity with no inclusion, and from varying the conductivity of the inclusion while maintaining a constant background conductivity of 1S/m.

To highlight the competing effects of EIT in the AEE measurement, Figure 3 shows ratio of the sum of the absolute value of the expected signal (which computes the Aee signal using the homogeneous EIT Jacobian and the true conductivity distribution) to the actual signal (heterogeneous EIT Jacobian and the true conductivity distribution) as well as the ratio of the peak AEE signal per pulse and the EIT measurement as a function of the conductivity.

4. Discussion

The model of the AEE signal given by 4 to 5 has two main implications. Firstly, since the signal is proportional to the EIT Jacobian, areas of a body with zero sensitivity for EIT should still have zero sensitivity in AET. Secondly, and more importantly, the effect of the EIT Jacobian competes with the AEE effect, washing out the naively expected σ dependence. Equation (7) reveals, to first order, an exact cancellation between the conductivity dependence of the AEE and the EIT sensitivity under the assumption of constant current flow. If this held to higher orders, the signal would be determined by the geometry of the target and the form of the pressure wave. In turn the reconstruction of the interior conductivity distribution based solely on a small number of direct AEE measurements (as opposed to using a larger number of measurements to reconstruct the boundary potential is in (Li *et al* 2020)) would be extremely difficult. Fortunately,

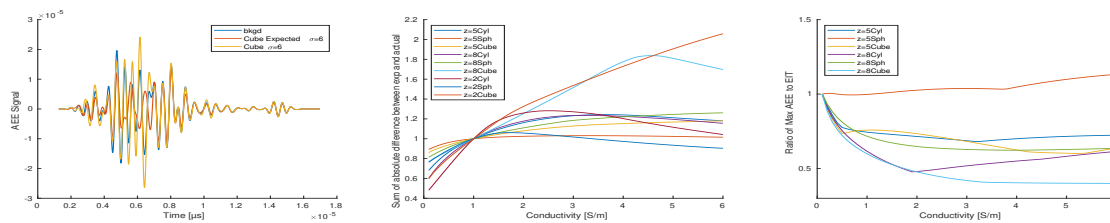


Figure 3: Left: An example of the differences between the expected (homogeneous Jacobian) and simulated (heterogeneous Jacobian) AEE signals. Middle: The ratio of the sum of the absolute value of the expected to actual AEE signals. Right: The ratio of the peak AEE signal to the EIT measurement as a function of changes in conductivity. The EIT in the denominator has been shifted up by 10 V to avoid a sign change which obscures the trend.

Figure 2 shows that while this washout effect does occur, it is hardly close to an exact cancellation. It is indeed the case that the EIT σ dependence overpowers the explicit σ dependence in the AEE coupling as can be clearly seen by the effect on the AEE signal in Figures 2. The signal is suppressed as the background conductivity increases but the rate of this suppression has a strong dependence on the EIT sensitivity (as the comparison between the different electrode placements and the different inclusions clearly demonstrate). The AEE sensitivity to the inclusion conductivity is not completely washed out though there is a suppression in signal when the pressure wave is maximally sensitive to the inclusion. As can be seen in Figure 3 there can be an enhancement relative to the naive expectation on the edge of the inclusion, which for some electrode placements can lead to an increase in the peak signal. The competition between suppression as the wave passes through the center of the inclusion and enhancement as it moves past the edge of the inclusion result in the different shapes seen for the cube ratio curves as edge effects are most significant for the cube. When we normalize the AEE signal to the unperturbed EIT signal, it can be seen that there is still a significant difference between the EIT and AEE signal's sensitivity to conductivity changes. This suggests that while the competition between EIT and AEE signals increases the difficulty of AET reconstructions using a small number of electrodes, a reconstruction relying on a minimal system with as few as two electrodes is achievable.

5. Conclusions

AET is a promising hybrid imaging method with the potential to overcome some of the limitations of EIT. To a good approximation, at a given point in space, the coupling between EIT and the US pressure wave has a linear dependence on the local pressure and the local conductivity and its effect can be modelled as a time dependent perturbation in the local conductivity. Given this linear dependence on σ , one would naively assume that the AEE signal is strongly dependent on the local values of the conductivity making it potentially feasible to reconstruct the conductivity using a small number surface of electrodes. However, the AEE's dependence on the conductivity is roughly cancelled by the measurement sensitivity of EIT, resulting in a partial suppression of the AEE signal as the local conductivity increases. While this cancellation is exact at first order and the EIT effects dominate the measurement's dependence on the conductivity, the AEE measurement is still sensitive to changes of the interior conductivity distribution, and as such conductivity reconstruction with minimal electrodes is still possible.

References

- Adesokan B J, Jensen B, Jin B and Knudsen K 2019 Acousto-electric tomography with total variation regularization *Inverse Problems* **35** 035008
- Ammari H, Bonnetier E, Capdeboscq Y, Tanter M and Fink M 2008 Electrical impedance tomography by elastic deformation *SIAM Journal on Applied Mathematics* **68**
- Jensen J and Svendsen N 1992 Calculation of pressure fields from arbitrarily shaped, apodized, and excited ultrasound transducers *IEEE Transactions on Ultrasonics, Ferroelectrics, and Frequency Control* **39** 262–267
- Jensen J 1996 Field: A program for simulating ultrasound systems *Medical and Biological Engineering and Computing* **34** 351–352
- Kuchment P and Kunyansky L 2010 Kunyansky, L.: 2d and 3d reconstructions in acousto-electric tomography. inverse probl. 27, 055013 *Inverse Problems* **27**
- Li C, An K, Zheng K and Lesselier D 2020 A complete framework for acousto-electric tomography with numerical examples *IEEE Access* **8** 98508–98517